Quantum-Mechanical Rate Equations for Semiconductor Lasers*

H. HAUG
Electrical Engineering Department, University of Wisconsin, Madison, Wisconsin 53706
(Received 4 February 1969)

Quantum-mechanical rate equations are derived for semiconductor lasers (SL). Fluctuation operators with shot-noise character describe the quantum nature of the transitions. These equations are treated in the high-temperature limit for pure and highly doped III-V compound semiconductors. Numerical calculations are carried out for GaAs. From the mean rate equations we determine (a) the temperature dependence of the threshold pump rate for pure bulk SL and the threshold current for SL junctions and (b) the temperature and pump dependences of the mean light intensity and of the mean quasi-Fermi-level. By linearizing the fluctuations around the mean values, the noise spectrum for the light intensity is obtained. The general form of the noise spectrum is the same as that obtained by McCumber for a four-level laser system. Above threshold a sharp resonance is found in the GHz region. The temperature and pump dependences of the spectrum and especially of the resonance frequency are calculated in detail. The results from the mean equations and from the noise calculations which are obtained for highly doped GaAs are compared with experimental results for junction lasers, and good agreement is found. For pure SL the present numerical results are in good agreement with former analytical results of Haug and Haken for the mean intensity and for the low-frequency part of the noise spectrum, which have been found for the regions below and above threshold. The results for pure bulk SL are applicable to experiments with optical or electron-beam excitation.

I. INTRODUCTION AND SUMMARY

THE noise spectrum for laser light was first calculated by McCumber[1] for a four-level laser system. Using rate equations with noise sources, a sharp resonance in the GHz region has been found. A quantum-mechanical justification of such an approach has been given by Lax.[2] Recently, the noise spectrum of semiconductor laser (SL) junctions has been studied experimentally[3] in the microwave region. Continuous oscillations with a frequency of a few GHz have been found both in the light intensity and in the junction current. The temperature and current dependences of this resonance frequency have been measured.

A theory, which is intended to predict the temperature and current dependences of the properties of the SL light output and current has to take into account a detailed description of the electron states and the distribution of the electrons over these states. The basic quantum-mechanical equations have already been developed[4] for the SL and have been used for a calculation of the low-frequency part of the noise spectrum both for the light intensity[5] and the junction current.[6] This approach did not, however, cover the immediate threshold region. The results for the intensity spectrum of SL light agreed with the result of a Hanbury Brown–Twiss experiment by Armstrong and Smith.[7] Recently, the low-requency spectrum for the junction current has also been measured[8] and an increase in the absolute noise spectrum was found at threshold, as predicted in Ref. 6. In this paper the rate-equation technique will be used in order to cover the full pump and frequency ranges, especially the immediate threshold region and the high-frequency part of the intensity noise spectrum. Furthermore, the temperature and pump dependences of the mean light output, of the mean population, and of the noise spectrum for the SL light intensity will be given a detailed numerical treatment. Recently, methods of continuous optical excitation have been developed[9] which allow a careful study of laser action in spatially homogeneous and, if desired, pure semiconductor bulk materials. In order to give predictions for such experiments, first optical band-to-band transitions in pure semiconductors will be treated. Most experimental data exist, however, for SL junctions with high doping levels. It is well known that the temperature dependence of the properties of these lasers is mainly determined by the impurity states,[10–12] i.e., by the changed optical matrix element and by the impurity bands or tails. The following model will be used. (a) No k-selection rule for the optical transitions, the matrix element is taken to be that for transitions between an acceptor level and the conduction-band edge; (b) the conduction band has an exponential tail in the density of states; (c) the acceptor band is a very narrow band (δ function for the density of states); and (d) no spatial variations are taken into account. This model gives simple analytical expressions, but it has the shortcoming that one has to

* Supported by the National Science Foundation (GK-1656).
[1] D. E. McCumber, Phys. Rev. **141**, 306 (1966).
[2] M. Lax, IEEE J. Quant. Electron. **3**, 37 (1967).
[3] L. A. D'Asaro, Sr., J. M. Cherlow, and T. L. Paoli, IEEE J. Quant. Electron **4**, 164 (1968).
[4] H. Haug, Z. Physik **200**, 57 (1967).
[5] H. Haug and H. Haken, Z. Physik **204**, 262 (1967).
[6] H. Haug, Z. Physik **206**, 163 (1967).
[7] J. A. Armstrong and A. W. Smith, Phys. Rev. **140**, A155 (1965).
[8] G. Guekos and M. J. O. Strutt, Electron. Letters **4**, 408 (1968).
[9] M. R. Johnson and W. Holonyak, Jr., J. Appl. Phys. **39**, 3977 (1968).
[10] G. Lasher and F. Stern, Phys. Rev. **133**, 533 (1964); F. Stern, *ibid.* **148**, 186 (1966).
[11] C. G. Dousmanis, H. Nelson, and D. L. Staebler, Appl. Phys. Letters **5**, 174 (1964).
[12] K. Unger, Z. Physik **207**, 332 (1967).

cut off the integral for the total spontaneous emission in the used high-temperature approximation. The numerical analysis is carried out for the example of pure and highly doped GaAs, but the techniques can readily be applied to all III-V compounds with a direct band gap. In II-IV compounds, laser action involves exciton states. A theory for stimulated phonon-assisted exciton recombination which describes the basic laser process in II-IV compounds has been developed in Ref. 13.

The SL electron-electron scattering processes bring the electrons in each band in a very short time into a quasi-Fermi distribution and excludes any hole-burning effects. As a direct consequence, only one single-laser mode is stable.[14] Another consequence is that it is sufficient to know the total number of electrons in one band. The two resulting quantum-mechanical rate equations for the number of photons N in the laser mode and for the total number of electrons N_C in one band are nonlinear equations for N and N_C. Both quantities are still operators. The quantum nature is contained in the fluctuation operators which have shot-noise character. As usual, a linearization procedure is used to solve the equations. The photon number is split into a mean value and the superimposed fluctuations. The fluctuations in the total number of electrons are expressed by fluctuations in the Fermi level.[6] The mean equations can be reduced in the high-temperature limit to two quadratic equations for the quasi-Fermi level of the upper band and for the photon number. These equations determine the temperature and pump dependences of both quantities. Quadratic equations are the simplest type of equations which can describe the saturation of the Fermi level and the typical strong change in the light intensity at threshold. It is shown that the simple analytical results given in Ref. 14 for the SL light intensity is an excellent approximation for $P_n \geq 1.02$, where P_n is the normalized pump rate, i.e., $P_n=1$ at threshold. The threshold currents which are obtained for the high-doping case are close in slope and magnitude to the curves which have been observed for SL junctions.[3,11] The noise spectrum has the structure which was first obtained by McCumber.[1] The resonance in the GHz region is very pronounced above threshold. The temperature and current dependences of the spectrum and especially of the resonance frequency are calculated. The shifts of the resonance with temperature and current agree in direction and order of magnitude with the experimental findings.[3] The present numerical results in the low-frequency part of the noise spectrum agree in the ranges of common validity with former analytical results[5] which have been obtained for the regions below and above threshold.

II. DERIVATION OF RATE EQUATIONS

The method of deriving the quantum-mechanical rate equations from the basic equations of motion for the system operators is well known.[2] In the case of the SL, the problem has already been solved for the number operators of the electrons in a paper dealing with the population and current noise.[6] In this paper, therefore, only a brief review of the assumptions and method will be given.

The equations of motion for the system operators contain unitary time-development terms and also irreversible terms due to the coupling to the heat baths.[15] These quantum-mechanical Langevin equations have been derived for the SL previously.[4] The photon amplitude $b^\dagger$ of the single-laser mode obeys the equation

$$(-i\omega+\kappa+d/dt)b^\dagger(t)=i\sum_{k_1k_2} g_{k_1k_2}{}^* a_{k_1C}{}^\dagger a_{k_2V}+F^\dagger(t), \quad (2.1)$$

where ω is the frequency of the empty cavity, κ is the loss constant, $F^\dagger$ is the fluctuation operator, and $g_{k_1k_2}$ is the optical matrix element between the state k_1C with wave vector k_1 in the upper band C (conduction band or its impurity tail) and the state k_2V of the lower band V (valence band or impurity band due to acceptors).

The time derivative of the dipole-moment operator $a_{k_1C}{}^\dagger a_{k_2V}$ is given by

$$(-i\epsilon_{k_1k_2}+\gamma_{k_1k_2}+d/dt)a_{k_1C}{}^\dagger a_{k_2V} = -ib^\dagger g_{k_1k_2}(n_{k_1C}-n_{k_2V})+F(t)_{k_1Ck_2V}, \quad (2.2)$$

where $\epsilon_{k_1k_2}=\epsilon_{k_1C}-\epsilon_{k_2V}$ is the frequency between k_1C and k_2V and $\gamma_{k_1k_2}$ is the damping constant, which is determined by all phase-destroying processes.

The time development of the number operator n_{kC} is given by

$$(d/dt)n_{k_1C}=\sum_{k_2}(-ibg^*{}_{k_1k_2}a_{k_1C}{}^\dagger a_{k_2V}+\text{H.c.}) -r_{sp,k_1}+p_{k_1}+F_{k_1Ck_1C}(t)+(d/dt)n_{k_1C}|_{el-el}, \quad (2.3)$$

where H.c. means the Hermitian conjugate of the preceding term.

$$r_{sp,k_1}=2\pi\hbar\sum_{k_2}|g_{k_1k_2}|^2\rho_L n_{k_1C}(1-n_{k_2V})$$

is the rate of spontaneous emission into the continuum of all light modes (except the laser mode), where ρ_L is the density of states for the light field. p_{k_1} is the pump rate. If one introduces pumping as a process which is the inverse of spontaneous emission, one gets p_{k_1}

[13] H. Haug and K. Grob, Phys. Letters **26A**, 41 (1967); H. Haug, J. Appl. Phys. **39**, 4687 (1968).

[14] H. Haug, Z. Physik **195**, 74 (1966). Based on these investigations, the multimode stabilization due to local inhomogeneities have been discussed by I. A. Poluectov, Yu. M. Popov, and N. N. Shuikin, in *Proceedings of the Ninth International Conference on the Physics of Semiconductors*, edited by S. M. Ryvkin (Nauka Publishing House, Leningrad, 1968) Vol. 1, p. 613; T. L. Paoli, J. R. Ripper, and T. H. Zachos, IEEE J. Quant. Electron. (to be published).

[15] The quantum-mechanical Langevin method has been developed by J. R. Senitzky, Phys. Rev. **119**, 670 (1960); **124**, 642 (1961); H. Haken, Z. Physik **190**, 327 (1966); M. Lax, Phys. Rev. **145**, 110 (1966).

$=2\pi\hbar\sum_{k_2}|p_{k_1k_2}|^2\rho_p n_{k_2V}(1-n_{k_1C})$, where $p_{k_1k_2}$ is the matrix element and ρ_p is the density of states for the pump field. $F_{k_1Ck_1C}$ is the fluctuation operator which is related to pumping and spontaneous emission. The last term describes the important electron-electron scattering processes. It also consists of a transition-rate term and a fluctuating term. The scattering processes bring the electron gas in very short time into quasiequilibrium, so that one can make the simplifying assumption that the electron gas is always nearly in a quasiequilibrium state. This fact has already been used in deriving the relaxation and fluctuation terms in (2.2) and (2.3). An equation similar to (2.3) holds for n_{k_2V}.

With the help of the fluctuation-dissipation theorem,[5] the second moments of the fluctuation operators have been calculated.

Using the identity $(d/dt)N=[(d/dt)b^\dagger]b+b^\dagger(d/dt)b$, one can write down the equation for the number operator of the photons. Its right-hand side depends on the dipole-moment operator $a_{k_1C}{}^\dagger a_{k_2V}$. Because γ which contains all phase-destroying processes is normally very large, one can solve (2.2) adiabatically.[2] Inserting the result in the equations of motion for N and n_{kC}, one finds equations which depend only upon number operators and fluctuation operators. If one splits the fluctuation operators into their mean values and the fluctuations around these mean values, the equation for the photon number operator has the following form:

$$(d/dt)N=-2\kappa N+E_{CV}+GN+F(t), \tag{2.4}$$

where

$$E_{CV}=\sum_{k_1k_2}|g_{k_1k_2}|^2 2\gamma_{k_1k_2} \times[(\epsilon_{k_1k_2}-\Omega)^2+\gamma_{k_1k_2}{}^2]^{-1}n_{k_1C}(1-n_{k_2V}) \tag{2.5}$$

is the rate of spontaneous emission into the laser mode, and Ω is the real laser frequency in the inverted crystal resonator. The gain is $G=E_{CV}-E_{VC}$, where E_{VC} is obtained from E_{CV} [Eq. (2.5)] by interchanging C and V. $F(t)$ has shot-noise character, i.e.,

$$\langle F(t)F(s)\rangle = \delta(t-s)(2\kappa N+\langle E_{CV}\rangle(N+1)+\langle E_{VC}\rangle N). \tag{2.6}$$

The averages $\langle\ \rangle$ in this paper are always averages over all heat baths, which have been coupled to the system to describe the nonunitary time development. As discussed in Ref. 4, one has to include for the semiconductor averages over the electron system itself because of the electron-electron relaxation process. In both (2.4) and (2.6), the contributions of the thermal photons are neglected.

Because of the assumption that the electrons in one band are always in a quasiequilibrium, one does not need the information about all individual occupation numbers. It is sufficient to have one equation for the total number of electrons in one band, $N_C=\sum_k n_{kC}$. If one sums the equation of motion for n_{kC} over all k values, the electron-electron terms drop out because they do not change the total number of electrons in one band. The resulting equation is

$$(d/dt)N_C=P-R_{sp}-GN-E_{CV}+F_C(t), \tag{2.7}$$

where $P=\sum_{k_1}p_{k_1}$ and $R_{sp}=\sum_{k_1}r_{sp,k_1}$ are the rates of pumping and spontaneous emission, respectively. The fluctuation operator again has shot-noise character:

$$\langle F_C(t)F_C(s)\rangle = \delta(t-s)\langle(P+R_{sp}+E_{CV}(N+1)+E_{VC}N)\rangle \tag{2.8}$$

and

$$\langle F(t)F_C(s)\rangle=\langle F_C(t)F(s)\rangle = -\delta(t-s)\langle(E_{CV}(N+1)+E_{VC}N)\rangle. \tag{2.9}$$

III. MEAN-RATE EQUATIONS

From the quantum-mechanical rate equations (2.4) and (2.7), the noise spectrum will be calculated by the usual linearization method.[1,2] One determines first the mean values $\bar N$, $\bar n_{kC}$, and $\bar n_{kV}$ and then takes small fluctuations around these values into account. One decomposes $N=\bar N+n(t)$. For the electrons, the expectation value of n_{kC} and n_{kV} are the quasi-Fermi distribution functions f_{kC} and f_{kV}. The fluctuations around these values can be expressed by a fluctuating Fermi level $\zeta(t)$. Only one quasi-Fermi level is used, because the quasi-Fermi levels in the upper and lower band are related and can be expressed in terms of one another.

$$\begin{pmatrix}n_{kC}(t)\\ n_{kV}(t)\end{pmatrix}=\begin{pmatrix}f_{kC}\\ f_{kV}\end{pmatrix}+\Delta\zeta(t)(\partial/\partial\zeta)\begin{pmatrix}f_{kC}\\ f_{kV}\end{pmatrix}. \tag{3.1}$$

The two equations for the mean stationary rates can then be written as

$$\bar P-\bar R_{sp}=2\kappa\bar N, \tag{3.2}$$

$$(2\kappa-\bar G)\bar N=\bar E_{CV}. \tag{3.3}$$

(The bars over all quantities in the following are omitted for convenience.)

The first task will be to determine the threshold and the laser frequency. In both examples which will be treated in the following sections, the functions E_{CV}, E_{VC}, and G have, in the high-temperature range ($|\zeta-\Delta|<kT$), the following form:

$$E_{CV}=e(\Delta)[1+(\zeta-\Delta)/2kT], \tag{3.4}$$

$$E_{VC}=e(\Delta)[1-(\zeta-\Delta)/2kT], \tag{3.5}$$

$$G=e(\Delta)(\zeta-\Delta)/kT, \tag{3.6}$$

where $\Delta=\hbar\Omega-E_g$ (E_g is the gap energy) is used to characterize the photon energy. The laser mode with the maximum gain will start to oscillate first, i.e.,

$$(d/d\Delta)G=0 \quad\text{or}\quad \zeta_{th}-\Delta=e/e'. \tag{3.7}$$

Neglecting at threshold the spontaneous emission rate into the laser mode, one obtains from (3.3)

$$2\kappa=G \quad\text{or}\quad \zeta_{th}=\Delta+2kT\kappa/e. \tag{3.8}$$

Combining the two last equations, one obtains

$$e^2/e' = 2kT\kappa, \tag{3.9}$$

which determines the laser frequency Δ as a function of T. Neglecting the term $2\kappa N$ in (3.2), which is still very small at threshold, one can calculate the threshold pump rate $P_{th}(T) = R_{sp}(\zeta_{th})$ by making use of the results of (3.9) and (3.8).

The next problem is to determine the average values N and ζ as functions of the pump rate P and the temperature T. The linear expansions (3.4)–(3.6) for E_{CV}, E_{VC}, and G in the high-temperature limit have been possible because one needs their values only at a fixed energy. But it is clear that such a linear expansion is not allowed for the spontaneous emission rate R_{sp}, which includes all electron states in both bands. Therefore, a different expansion will be used. The Fermi level will saturate above threshold in the case of spatial and energetic homogenization which is treated here. The analysis will show that the Fermi level will asymptotically approach the value ζ_{th} above threshold. As one is interested mainly in the threshold and lasing regions, it is a good approximation to use a linear expansion of the spontaneous emission rate R_{sp} around the threshold value ζ_{th}.

$$R_{sp}(\zeta) = R_1(\zeta_{th}) + R_2(\zeta_{th})(\zeta - \zeta_{th})/kT, \tag{3.10}$$

where R_1 and R_2 are determined by numerical integration for a given temperature. The same expansion is used for the total number N_C of electrons in the upper band:

$$N_C(\zeta) = N_1(\zeta_{th}) + N_2(\zeta_{th})(\zeta - \zeta_{th})/kT. \tag{3.11}$$

Starting with Eq. (3.3) and inserting the expansions (3.4)–(3.6), one gets

$$\zeta = (2N\zeta_{th} + \Delta - 2kT)/(2N+1), \tag{3.12}$$

or

$$N = (\zeta - \Delta + 2kT)/(\zeta_{th} - \zeta). \tag{3.13}$$

These equations show already that $\zeta < \zeta_{th}$; only for $N \to \infty$ does $\zeta \to \zeta_{th}$.

Using these results and Eq. (3.2), one finds quadratic equations for N and ζ:

$$\zeta^2 + 2\zeta[(R_1 - P - \kappa)kT/R_2 - \zeta_{th}] = -\zeta_{th}^2 + (kT/R_2)[2\kappa(2kT - \Delta) - \zeta_{th}(P - R_1)] \tag{3.14}$$

and

$$4\kappa N^2 + 2N(\kappa + R_1 - P) = P - R_1 - (R_2/kT)(\zeta_{th} + \Delta - 2kT). \tag{3.15}$$

If R_1 and R_2 are known, one can calculate $N(P,T)$ and $\zeta(P,T)$ from these equations. A quadratic equation for N and ζ is the simplest form which is still able to describe the pronounced changes within the threshold region.

In the limit below, threshold ($P < R_1$ and N still small) Eq. (3.15) gives

$$N = [R_2/(R_1 - P)](\zeta_{th} - \Delta + 2kT)/kT - 1. \tag{3.16}$$

The approximate value of ζ in this region can best be obtained from (3.2) directly by neglecting $2\kappa N$:

$$\zeta = \zeta_{th} - (kT/R_2)(R_1 - P). \tag{3.17}$$

These results show the increase of N and ζ below threshold. One sees that the results have no validity far below threshold, because the assumption $(\zeta - \zeta_{th})/kT < 1$ does not hold in this region. But in the range $0.5 < P/R_1 < 0.98$ the limiting results are very good approximations.

Well above threshold ($P/R_1 > 1.04$), the limiting result for the photon number is $N = (P - R_1)/2\kappa$. From (3.12) one finds for $\zeta - \zeta_{th} \ll kT$, $\zeta = \zeta_{th} - [\kappa/(P - R_1)] \times (2kT - \Delta)$. Because $\kappa/R_1 \simeq 10^{-7}$, the slope of $N(P)$ above threshold is much larger than that below threshold. Because of the same reason, one cannot see a difference between ζ and ζ_{th} in a plot of $\zeta(P)$ above threshold. (See, for instance, Fig. 2.)

IV. NOISE

In the last section the mean stationary rate equations were solved. Following the analysis of McCumber[1] one now treats the fluctuations around the mean values. Using $(d/dt)N_c = (d/d\zeta)N_C(d/dt)\zeta$, one obtains the following linearized equations:

$$(d/dt)\Delta\zeta = -\Lambda_{\zeta\zeta}\Delta\zeta - \Lambda_{\zeta n}n + F_\zeta, \tag{4.1}$$

$$(d/dt)n = -\Lambda_{n\zeta}\Delta\zeta - \Lambda_{nn}n + F, \tag{4.2}$$

where

$$\Lambda_{\zeta\zeta} = (R_2 - kT\Lambda_{n\zeta})/N_2,$$
$$\Lambda_{\zeta n} = kTG/N_2,$$
$$\Lambda_{n\zeta} = -e(2N+1)/2kT,$$
$$\Lambda_{nn} = 2\kappa - G,$$

and $F_\zeta = (kT/N_2)F_C$. No pump fluctuations have been included. Introducing a Fourier transform $A(t) = \int A_\omega e^{i\omega t} d\omega$ for $\Delta\zeta$, n, F, and F_ζ, one gets a system of two linear equations for $\Delta\zeta_\omega$ and n_ω. Solving (4.1) and (4.2) for the light field, one finds for the noise spectrum

$$\langle |n_\omega^2| \rangle = \frac{\langle |F_\omega|^2 \rangle \Lambda_{\zeta\zeta}^2 - 2\Lambda_{\zeta\zeta}\Lambda_{n\zeta}\langle |F_\omega F_{\zeta\omega}| \rangle + \langle |F_{\zeta\omega}|^2 \rangle \Lambda_{n\zeta}^2 + \omega^2 \langle |F_\omega|^2 \rangle}{(\Lambda_{nn}\Lambda_{\zeta\zeta} - \Lambda_{\zeta n}\Lambda_{n\zeta} - \omega^2)^2 + \omega^2(\Lambda_{nn} + \Lambda_{\zeta\zeta})^2}. \tag{4.3}$$

Here the notation of Lax[2] is used:

$$\langle|n_\omega|^2\rangle=\int dt\langle n(0)n(t)\rangle e^{i\omega t}=S(\omega). \tag{4.4}$$

The relation $\langle n_\omega n_{\omega'}\rangle=2\pi\delta(\omega-\omega')\langle|n_\omega|^2\rangle$ holds. From these definitions and (2.6), (2.8), and (2.9), one finds

$$\langle|F_\omega|^2\rangle=2\kappa N+E_{CV}(N+1)+E_{VC}N, \tag{4.5}$$

$$\langle|F_{\zeta\omega}|^2\rangle=(kT/N_2)^2 \times(P+R_{sp}+E_{CV}(N+1)+E_{VC}N), \tag{4.6}$$

$$\langle|F_{\zeta\omega}F_\omega|\rangle=\langle|F_\omega F_{\zeta\omega}|\rangle =-(kT/N_2)(E_{CV}(N+1)+E_{VC}N). \tag{4.7}$$

The spectrum is of the form

$$y(\omega)=\frac{A^3+B\omega^2}{(a^2-\omega^2)^2+b^2\omega^2}. \tag{4.8}$$

The structure of the denominator causes a sharp resonance above threshold. Around the resonance frequency $\omega_0=a$, one can approximate the spectrum by

$$y(\omega)\simeq\frac{4(A^3/\omega_0^2+B)}{(\omega-\omega_0)^2+(\frac{1}{2}b)^2}, \tag{4.9}$$

where

$$\omega_0=(\Lambda_{nn}\Lambda_{\zeta\zeta}-\Lambda_{\zeta n}\Lambda_{n\zeta})^{1/2}. \tag{4.10}$$

The half-width is

$$2\gamma=b=\Lambda_{nn}+\Lambda_{\zeta\zeta}. \tag{4.11}$$

The resonance frequency ω_0 is in the GHz region. In the following especially the pump and temperature dependences of the spectrum and of the resonance frequency will be discussed. Solving the Eqs. (4.1) and (4.2) for $\Delta\zeta_\omega$, one finds for $\langle|\Delta\zeta_\omega|^2\rangle$ a result with the same resonance denominator. This explains why the resonances in the noise spectrum are observable simultaneously in the light field and in the junction current of a laser diode.[3]

V. NUMERICAL CALCULATIONS FOR PURE GaAs

In pure semiconductor materials with a direct band gap, the k selection for band-to-band transitions is valid, i.e., $g_{k_1k_2}=\delta_{k_1k_2}g$. For $\hbar\gamma\ll kT$, ζ, Δ, the expression (2.5) for the rate of spontaneous emission into the laser mode reduces to

$$E_{CV}=A\Delta^{1/2}f_C(1-f_V), \tag{5.1}$$

where $A=2\pi\hbar\rho'|g|^2$. The factor ρ' of the density of states for parabolic bands is $\rho'=V(2m_r^3)^{1/2}/(\pi^2\hbar^3)$, where V is the volume, and m_r is the reduced mass ($m_r^{-1}=m_C^{-1}+m_V^{-1}$). The absolute square of the matrix elements is[16,17]

$$|g|^2=\frac{\pi e^2}{6V\eta^2m_C}\frac{(E_g/\hbar\Omega)(E_g+\sigma)}{E_g+\frac{2}{3}\sigma}, \tag{5.2}$$

where η is the index of refraction and σ is the spin-orbit splitting. The quasi-Fermi distributions are

$$f_C=(1+e^{(\Delta-\zeta)\alpha/kT})^{-1} \quad\text{and}\quad f_V=(1+e^{(\zeta-\Delta)\beta/kT})^{-1},$$

with $\alpha=m_r/m_C$ and $\beta=m_r/m_V$.

The high-temperature approximation then gives the form (3.4) with $e(\Delta)=\frac{1}{4}A\Delta^{1/2}$. From (3.9) and (3.8), one gets $\Delta=(4\kappa kT/A)^{2/3}$ and $\zeta_{th}=3\Delta$. Knowing $\zeta_{th}(T)$, one can numerically determine the threshold pump rate:

$$P_{th}=R_1=2\pi\hbar\int_0^\infty\rho_L\rho'|g|^2f_C(1-f_V)dE, \tag{5.3}$$

where $\rho_L=VE_g^2\eta^3/2\pi^2\hbar^3c^3$. The variation of ρ_L with E is neglected. Equation (5.3) can be written as

$$R_1=A\rho_L(kT)^{3/2}\int_{-3\Delta/kT}^\infty J(x)dx, \tag{5.4}$$

where

$$J(x)=(x+3\Delta/kT)^{1/2}(e^x+e^{\alpha x}+e^{\beta x}+1)^{-1}. \tag{5.5}$$

Similarly, $R_2=kT(d/d\zeta_{th})R_1$ is given by

$$R_2=A\zeta_L(kT)^{3/2}\int_{-3\Delta/kT}^\infty J(x) \times[\alpha(1+e^{-\alpha x})^{-1}+\beta(1+e^{-\beta x})^{-1}]dx. \tag{5.6}$$

The integrals are calculated using the following parameter values.[16] $\eta=3.5$, $m_C=0.072m$, $m_V=0.5m$, $E_g=1.437$ eV, $\sigma=0.33$ eV, and $\kappa=10^{11}$ sec^{-1}. The volume was taken to be $V=10^{-8}$ cm.^{3}

R_1 is given in Fig. 1. The result can be represented by $P_{th}=R_1=P_0T^{1.44}$, where $P_0=8.8\times10^{14}$ °K$^{-1.44}$/sec. This shows that the temperature dependence of the integral in (5.4) is very weak. The approximate result $P_{th}\propto T^{3/2}$

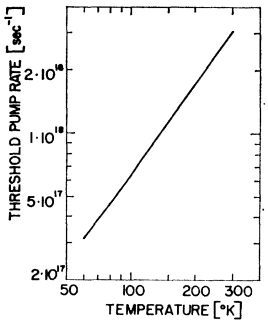

FIG. 1. Threshold pump rate versus temperature for a pure GaAs crystal with a volume of 10^{-8} cm^{-3}.

[16] O. Madelung, *Physics of III-V Compounds* (John Wiley & Sons, Inc., New York, 1964).

[17] H. Haug, Z. Physik 194, 482 (1966). On the right-hand side of formula (21) a factor of $\frac{1}{12}$ is missing.

was first obtained by Hall[18] for pure semiconductors, showing that the temperature dependence of the threshold current of junction lasers has to be determined by impurity states. Similar integrations are carried out to obtain $R_2(T)$, $N_1(T)$, and $N_2(T)$.

The mean rate equations can now be solved numerically. Figure 2 gives the pump dependence of the Fermi level ζ. As discussed in Sec. IV, the change at threshold is not abrupt as it appears in the plot because of the small ratio of κ/R_1. From the Fermi level one can calculate the gain function. The gain function saturates above threshold, i.e., it approaches asymptotically the value 2κ (Fig. 3). The unsaturated gain G_{uns}, which is obtained by extrapolating the gain from below threshold into the region above threshold, has been used in former formulations of the SL theory.[5,14]

Figure 4 shows the photon number versus the pump rate. The laser light output $2\kappa\hbar\Omega N$ changes in the threshold region by five orders of magnitude. Experimental

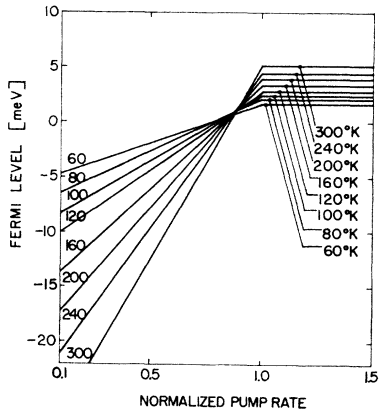

FIG. 2. Quasi-Fermi level versus normalized pump rate P_n for pure GaAs at various temperatures.

curves for optically pumped homogeneous GaAs crystals[19] show the same amount of increase in the threshold region, but the slopes are normally not quite as steep as the theory predicts.

In Ref. 12 it was shown that above threshold the photon number N in the laser mode is given by

$$2\kappa = G_{\text{uns}}/(1+aN) \tag{5.7}$$

(Note that the definitions of the gain of this paper and of Refs. 4, 5, and 12 differ by a factor of 2.) Using the unsaturated gain G_{uns} from Fig. 3 one can show that (5.7) is an excellent approximation for $P_n > 1.02$. The saturation constant a is found to be

$$a = 3.85\times 10^{-4} T^{-1.12}\ ^\circ\text{K}^{1.12} \tag{5.8}$$

for the used volume of $V = 10^{-8}$ cm^3. If one works with

[18] R. N. Hall, Solid-State Electron. 6, 405 (1963).

[19] N. G. Basov, A. Z. Grasyuk, V. F. Ehfimkov, and Kamulin, Fiz. Tverd. Tela 9, 88 (1967) [English transl.: Soviet Phys.—Solid-State 9, 65 (1967)].

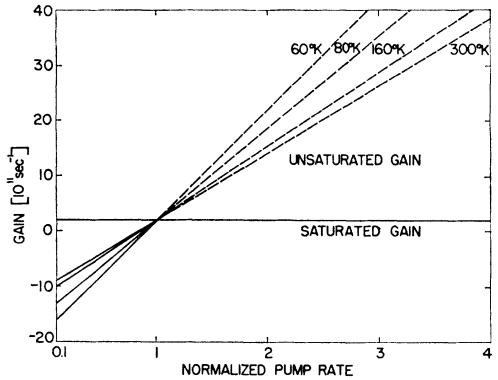

FIG. 3. Gain $G = E_{CV} - E_{VC}$ versus normalized pump rate P_n for pure GaAs at various temperatures. The unsaturated gain G_{uns} is obtained by extrapolation.

the photon density N/V instead of N, the constant $aV = 3.85\times 10^{-12} T^{-1.12}$ cm^3 °K$^{1.12}$ is volume-independent. The formula (5.8) holds very precisely in the range 60–300°K. The linearized version of (5.7) $2\kappa = G_{\text{uns}} \times (1-aN)$ fails, however, very early, i.e., for $P_n > 1.06$, because aN soon starts to become comparable to 1.

The noise spectrum $S(\omega)$ can now be calculated for various pump levels and temperatures. In Fig. 5 the relative noise spectrum $S_n(\omega) = S(\omega)/N^2$ is plotted versus the linear frequency $f = \omega/2\pi$ for 80°K. The parameter values give the normalized pump rates for the various curves. One sees that, starting at threshold, a resonance in the GHz region builds up which becomes very pronounced and sharp immediately above threshold. The resonance frequency shifts toward higher frequencies as the pump rate is increased at a constant temperature (Fig. 6). An increase in temperature at

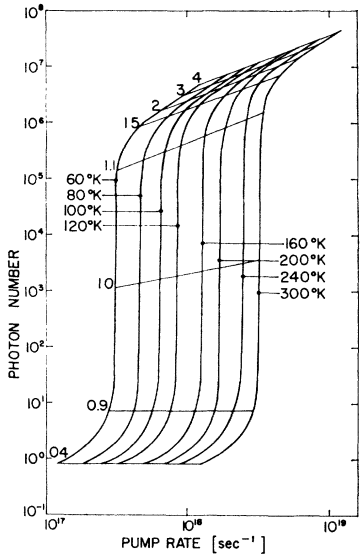

FIG. 4. Photon number in the laser mode versus absolute pump rate P for pure GaAs at various temperatures. The numbers 0.4 to 4 give the values of the normalized pump rate P_n.

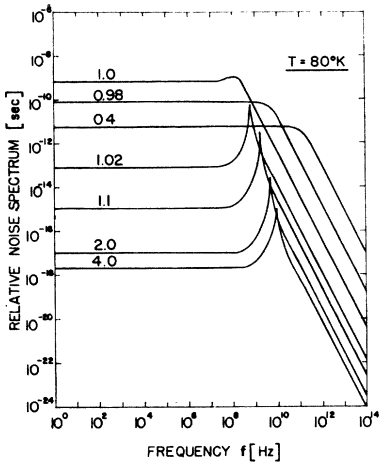

FIG. 5. Relative noise spectrum $S_n(\omega)$ versus linear frequency f for pure GaAs at 80°K and various normalized pump rates.

constant pump rate decreases the resonance frequency. The noise spectrum and especially the GHz resonances have not yet been studied experimentally in pure homogeneous semiconductors. In Fig. 7 the relative noise spectrum for zero frequency is plotted versus the photon number N. The dashed lines give the results of Ref. 5, which have been obtained by quasilinearization procedures directly from the amplitude equations (2.1)–(2.3). The result for the noise spectrum below threshold was $S_n(\omega=0)=(\kappa-\frac{1}{2}G)^{-1}$, and above threshold, $S_n(\omega=0)=[(1+aN)^2/a^2N^3]E_{CV}/2\kappa^2)$. But the linearization procedure did not allow coverage of the threshold region $0.99\leq P_n\leq 1.01$. The difference far below threshold exists because the present method fails in that region; the difference far above threshold arises because

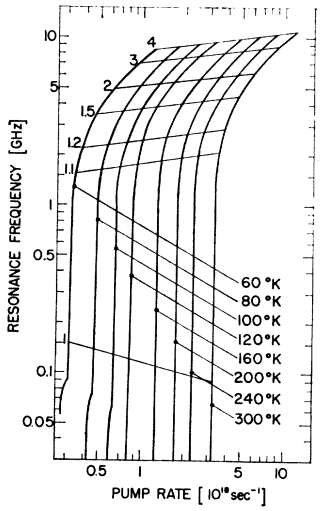

FIG. 6. Resonance frequency f_{max} versus absolute pump rate for pure GaAs at various temperatures. The values of relative pump values P_n are also given.

in Ref. 5 the electron population fluctuations have not been included.

VI. NUMERICAL CALCULATIONS FOR HIGHLY DOPED GaAs

In p-n junctions high doping levels are used. To compare the theory with experimental data taken with junction lasers, one has to treat transitions between impurity bands. To keep the numerical work at a reasonable level, the following model will be used. For the upper band an exponential density of states $\rho_C=\rho_0 e^{E/E_0}$ is assumed, where one takes both for ρ_0 and E_0 numbers which have been found experimentally.[11] The lower band is assumed to be a sharp acceptor level with a density of states $\rho_V=Z\delta(E_V-\bar{E})$. The origin of the energy coordinate is in the upper band at $E_C=0$. For the matrix

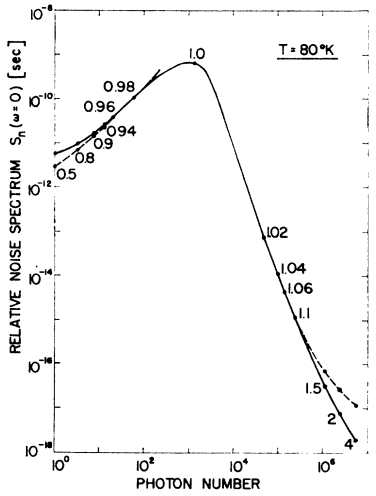

FIG. 7. Low-frequency limit of the relative noise spectrum versus photon number for pure GaAs at 80°K. The parameters along the curve give the normalized pump rate P_n. The dashed curves are analytical results of Ref. 5.

element the result of Ref. 20 is used, which has been calculated for a donor-to-conduction-band transition. As in the calculations of Lasher and Stern,[10] any dependence on k is neglected, i.e., $g_{k_1k_2}=h$, where $|h|^2=(64\pi a^{*3}/V)|g|^2$ with $a^*=\epsilon_0(m/m^*)a_0$, a_0 is the Bohr radius of a hydrogen atom, ϵ_0 is the static dielectric constant, m^* is the effective mass of the acceptor electron, and g is the band-to-band matrix element (5.2). For this model the rate of spontaneous emission into the laser mode is

$$E_{CV}=|h|^2 2\pi\hbar Z\rho_0 e^{\Delta/E_0} f_C(1-f_V), \qquad (6.1)$$

where $f_C=(1+e^{(\Delta-\zeta)/kT})^{-1}$ and

$$f_V=(1+\tfrac{1}{2}e^{(\bar{E}-\zeta_V)/kT})^{-1}.$$

Note that the Fermi distribution f_V holds if an acceptor atom of the group II (e.g., Zn) replaces Ga^{+3}. The for-

[10] O. M. Eagles, Phys. Chem. Solids 16, 76 (1960).

mula equals that for a donor of group V inserted into a material of group-IV atoms.

The energy Δ is given by $\Delta=\hbar\Omega-\bar{E}$. Because the density of the valence band which lies close to the acceptor level is a very rapidly rising function with energy, the changes in ζ_V will be small. As a simplifying assumption, $f_V=\frac{1}{2}$ is used. Then the high-temperature expressions[21] have again the form (3.4)–(3.6), with $e(\Delta)=Be^{\Delta/E_0}$, where $B=\frac{1}{2}\pi\hbar Z\zeta_0|h|^2$, which is valid for $|\Delta-\zeta|<kT$. The laser frequency is, according to (3.9), $\Delta=E_0\ln(2\kappa kT/BE_0)$ and the threshold Fermi level $\zeta_{\rm th}=E_0+\Delta$ [see (3.8)].

The integral of the total spontaneous emission rate can be written as

$$R_1=2B\rho_L\int_{-\infty}^{\infty}dE\,e^{E/E_0}(1+e^{(E-\zeta_{\rm th})/kT})^{-1}. \quad (6.2)$$

This integral converges only for $E_0>kT$, but not in the high-temperature limit. The exponential density of states, which does not include the bending over into a square-root law, is an oversimplification. Also the k dependence of the matrix element which was neglected would help to assure convergence of the integral. For the pure exponential tail, one has to cut off the integral at $E=\zeta_{\rm th}+2kT$. This is the energy at which the linearized Fermi distribution reaches zero. In the Appendix it is shown that the integral R_1 (as well as R_2, N_1, and N_2) can be calculated explicitly by using an integral representation[22] of the Fermi distribution. The result is

$$R_1=2B\rho_L E_0 e^{\zeta_{\rm th}(T)/E_0}\left(\frac{\pi x}{\sin\pi x}-xe^{2x}\sum_{n=1}^{\infty}\frac{e^{-2n}(-1)^n}{(x-n)}\right), \quad (6.3)$$

where $x=kT/E_0$. Similar expressions are obtained for R_2, N_1, and N_2 [Eq. (A9)]. The threshold pump rate is $P_{\rm th}=R_1$ and the threshold current in a junction laser is $i_{\rm th}=eP_{\rm th}/\eta'$, where η' is the quantum efficiency. The following parameters have been used for the numerical evaluations.[10,11,16]

$$V=1.2\times10^{-8}\ \text{cm}^3=15\times2\times400\times10^{-12}\ \text{cm}^3,$$

where 2×10^{-4} cm is the junction width. The volume is typical for junctions with stripe geometry.[23] $E_0=10$ meV, except for Fig. 8 where $E_0=5$, 10, 12, and 20 meV. $\rho_0/V=5\times10^{18}\ \text{cm}^{-3}\ \text{eV}^{-1}$. The donor impurity concentration is taken to be $Z=10^{18}\ \text{cm}^{-3}$. The static dielectric constant is $\epsilon_0=12.5$, and the mass of the acceptor electron is $m^*=0.39m$; this gives an effective Bohr radius for the acceptor of $a^*=16.95\times10^{-8}$ cm. For the quantum efficiency a value of $\eta'=\frac{1}{2}$ is assumed.

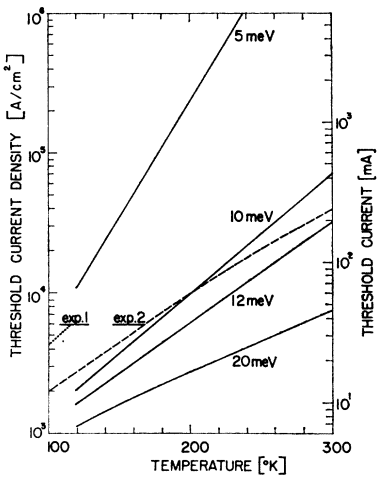

FIG. 8. Threshold current density versus temperature for various values of the characteristic energy E_0 of the band tail. The dotted and dashed lines are experimental curves given in Refs. 3 and 11. The right scale gives the values of the threshold current in mA.

The rest of the parameters are the same as in Sec. V. In Fig. 8 the threshold current versus temperature for various values of E_0 is given. The results confirm earlier qualitative discussions,[11] which assumed that an exponential density of states in the upper band would result in an essentially exponential dependence of the threshold current on temperature. E_0 increases with increasing n-type doping. Two experimental curves which have been obtained by two research groups[3,11] are given for comparison. These curves have slopes similar to the theoretical curves for $E_0=10$ or 12 meV. In the following only $E_0=10$ meV will be used. Figure 9 gives the photon number versus the normalized pump rate, and Fig. 10 shows the pump dependence of the Fermi level in the impurity band.

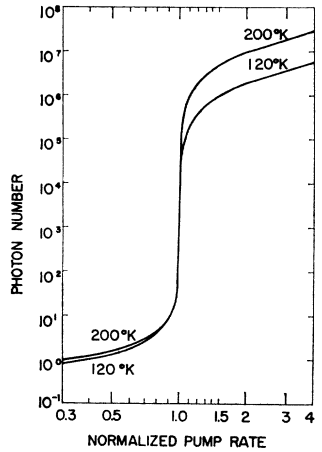

FIG. 9. Photon numbers in the laser mode versus normalized pump rate for highly doped GaAs at 120 and 200°K.

[21] This model has also been used by N. G. Basov, V. N. Morozov, V. V. Nikitin, and A. S. Semonov, Soviet Phys.—Semiconductors 1, 1305 (1968).

[22] A. Wasserman, Phys. Letters 27A, 360 (1968), and references therein.

[23] J. C. Dyment and L. A. D'Asaro, Appl. Phys. Letters 11, 292 (1967).

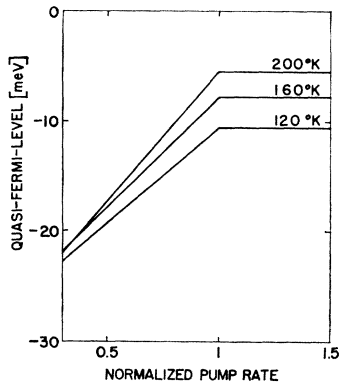

FIG. 10. Quasi-Fermi level versus normalized pump rate for highly doped GaAs at 120, 160, and 200°K.

The absolute noise spectrum $S(\omega)$ is plotted in Fig. 11 for $T=120°K$. The sharp resonances in the GHz region reach a maximum at a normalized pump rate of $P_n\simeq 1.65$. There the maximum value is about 5×10^3 times larger than the low-frequency plateau.

These resonances were first found for SL in noise measurements around pump values of $P_n\gtrsim 2$ as continuous oscillations with a linewidth of approximately 10 MHz.[3] Recently the resonances have been observed in the region $1.0<P_n<2$ as broader peaks.[24] It seems that these fluctuations somehow trigger, for $P_n>2$, a process which gives rise to the observed continuous oscillations with the small linewidth of 10 MHz. (See note added in proof.) Using the approximate formula for the linewidth [Eq. (4.11)] one finds that at $T=120°K$ the full half-width in linear frequency is $2\gamma/2\pi=136$, 270, 360, 590, and 820 MHz for $P_n=1.02$, 1.6, 2, 3, and 4.

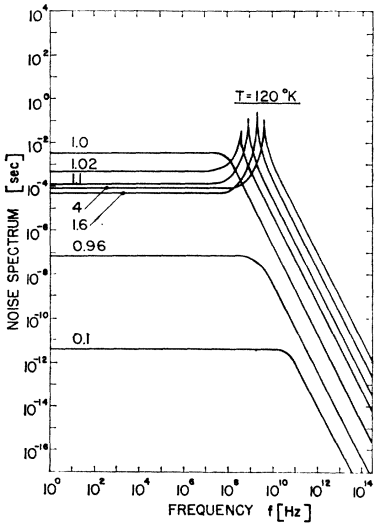

FIG. 11. Absolute noise spectrum versus linear frequency f for highly doped GaAs 120°K and various normalized pump rates.

[24] T. L. Paoli (private communication).

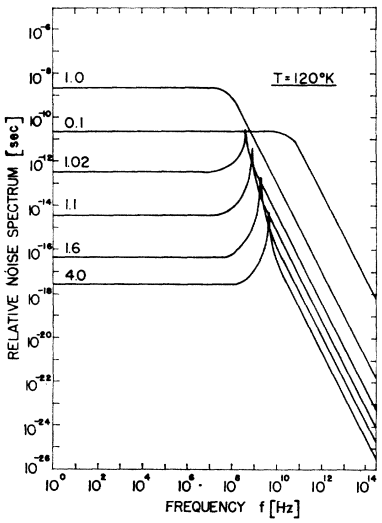

FIG. 12. Relative noise spectrum $S_n(\omega)$ versus linear frequency f for highly doped GaAs at 120°K and various normalized pump rates.

The resonances have also been studied by modulating the junction current in the microwave frequency range.[25]

The relative noise spectrum $S_n(\omega)=S(\omega)/N^2$ is plotted in Fig. 12 again for 120°K. The curves show the rapid decrease of the relative intensity fluctuations above thresholds. The shift of the resonance frequency with pump rate is given for $T=120$, 160, and 200°K (Fig. 13). The high-temperature approximation is only valid for $T\geq 120°K$. By extrapolating one obtains a

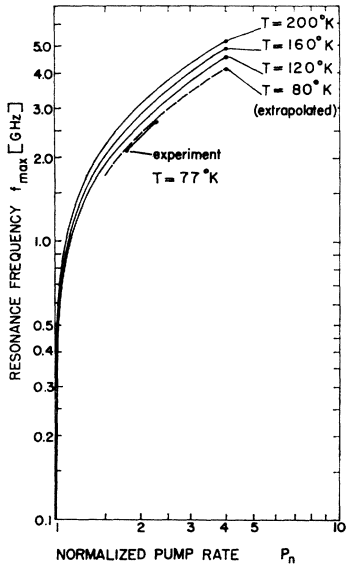

FIG. 13. Resonance frequency f_{max} versus normalized pump rate P_n for highly doped GaAs at 120, 160, and 200°K. The dashed line for 80°K is obtained by extrapolation. The experimental curve is taken at 77°K. (See Ref. 3.)

[25] T. Ikegami and Y. Suematsu, IEEE J. Quant. Electron. 4, 148 (1968).

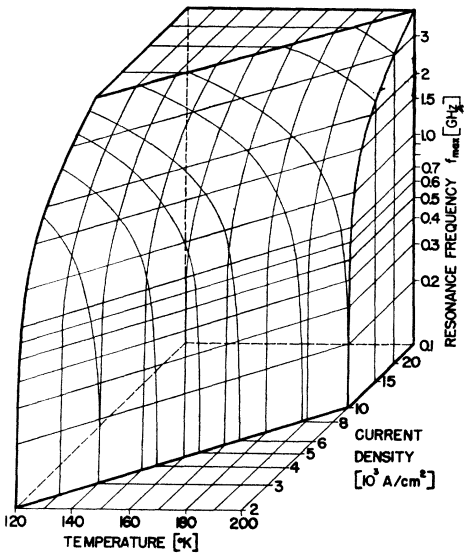

FIG. 14. Resonance frequency f_{max} versus current density and temperature for highly doped GaAs. The various curves are obtained by keeping one of the three quantities constant.

curve for 80°K which is, in slope and magnitude, very close to the curve obtained at 77°K by d'Asaro, Cherlow, and Paoli.[3] The dependence of the resonance frequency on both the temperature and the current can clearly be seen in a three-dimensional plot (Fig. 14). At a constant temperature of 120°K, the plot shows an increase of approximately 9 MHz/mA with increasing current, while for constant currents the curves decrease with increasing temperature with roughly 50 MHz/°K. Experimentally[3] one finds an increase of 15 MHz/mA at constant temperature and a decrease of 150 MHz/°K at constant current.

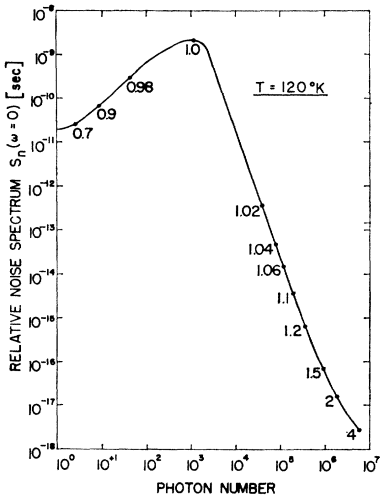

FIG. 15. Low-frequency limit of the relative noise spectrum versus photon number for highly doped GaAs at 120°K. The normalized pump rates are given.

In Fig. 15 the relative noise spectrum at zero frequency $S_n(\omega=0)$ is given for $T=120$°K. The slopes of the curve on both sides near the maximum at threshold agree with the slopes of the experimental curve which has been obtained by Armstrong and Smith in a Hanbury Brown–Twiss experiment at 4°K.[7] Recently, Gukeos and Strutt[8] reported similar measurements over a larger pump range. They observed a series of noise maxima with increasing pump rate which can be interpreted as being the noise maxima of the successive thresholds of various lasing filaments.

Note added in proof. In the meantime T. L. Paoli and J. E. Ripper (to be published) proposed that the noise peak drives an oscillation with a frequency which corresponds to the difference in frequency separation between three adjacent longitudinal modes.

ACKNOWLEDGMENT

The author appreciates a discussion with Dr. Paoli (Bell Telephone Laboratories, Murray Hill, N. J.) about the connections between the results of this paper and his experimental findings.

APPENDIX

For doped semiconductors the integrals R_1, N_1, R_2, N_2, which are defined in (3.10) and (3.11), will be calculated. According to (6.2), $R_1=2B\rho_L I_1(\zeta=\zeta_{th})$, where

$$I_1=\int_{-\infty}^{a} dE e^{E/E_0}(1+e^{(E-\zeta)/kT})^{-1}. \quad \text{(A1)}$$

The cutoff energy is $a=\zeta_{th}+2kT$. $R_2=2B\rho_L I_2$ is the derivative of R_1, or $I_2=kT\partial/\partial\zeta I_1|_{\zeta=\zeta_{th}}$; furthermore $N_1=\rho_0 I_1$ and $N_2=\rho_0 I_2$. So one has to evaluate only I_1. Introducing $\epsilon=(a-E)/kT$, with $a-\zeta>0$, one obtains from

$$I_1=kTe^{a/E_0}\int_0^{\infty} d\epsilon\, e^{-\epsilon kT/E_0}(1+e^{-\epsilon+(a-\zeta)/kT})^{-1}. \quad \text{(A2)}$$

It is convenient to write this as a contribution of a band which is completely filled up to a, minus the contribution of the missing electrons.

$$I_1=E_0e^{a/E_0}-kTe^{a/E_0}\int_0^{\infty} d\epsilon \times e^{-\epsilon kT/E_0}(1+e^{\epsilon-(a-\zeta)/kT})^{-1}. \quad \text{(A3)}$$

Now an integral representation of the Fermi distribution[22] is used:

$$I_1-E_0e^{a/E_0}=-\frac{kTe^{a/E_0}}{2\pi i}\int_{c-i\infty}^{c+i\infty}\frac{dZ\pi}{\sin(\pi Z)} \times\int_0^{\infty} d\epsilon\, e^{-\epsilon kT/E_0-Z[\epsilon-(a-\zeta)/kT]}. \quad \text{(A4)}$$

where $0<c<1$. After integrating over ϵ, one finds for the right-hand side

$$-\frac{kTe^{a/E_0}}{2\pi i}\int_{c-i\infty}^{c+i\infty}\frac{dZ\,\pi}{[\sin(\pi Z)(Z+kT/E_0)]}e^{Z(a-\zeta)/kT}. \quad \text{(A5)}$$

Because $a-\zeta>0$, we close the contour integral by a circle to the left in the complex Z plane. Summing up the contributions of all residues, one gets

$$I_1-E_0e^{a/E_0}=kTe^{a/E_0}\left(\frac{\pi e^{(\zeta-a)/E_0}}{\sin(\pi kT/E_0)}-\sum_{n=0}^{\infty}\frac{(-1)^n e^{-n(a-\zeta)/kT}}{kT/E_0-n}\right). \quad \text{(A6)}$$

One can easily see that the singularities on the right-hand side of (A6) for $n\rightarrow kT/E_0$ cancel. Setting $\zeta=\zeta_{\rm th}$, one finds, with $x=kT/E_0$,

$$I_1=E_0e^{\zeta_{\rm th}/E_0}\left(\frac{\pi x}{\sin\pi x}-xe^{2x}\sum_{n=1}^{\infty}\frac{(-1)^n e^{-2n}}{x-n}\right). \quad \text{(A7)}$$

Using (A6), one gets

$$I_2=E_0e^{\zeta_{\rm th}/E_0}\left[\frac{\pi x^2}{\sin\pi x}-xe^{2x}\sum_{n=1}^{\infty}\frac{(-1)^n ne^{-2n}}{x-n}\right], \quad \text{(A8)}$$

which can also be written as

$$I_2=xI_1-xE_0e^{2x+\zeta_{\rm th}/E_0}/(1+e^2). \quad \text{(A9)}$$

The formulas (A7) and (A9) are used in a computer program to evaluate R_1, R_2, N_1, and N_2 as functions of temperature.

PHYSICAL REVIEW VOLUME 184, NUMBER 2 10 AUGUST 1969

Ultraviolet-Absorption Spectra of Europium and Ytterbium in Alkaline Earth Fluorides*

EUGENE LOH
Physical Sciences Department, McDonnell Douglas Astronautics Company, Western Division, Santa Monica, California 90406

(Received 3 February 1969)

The ultraviolet-absorption spectra of europium and ytterbium ions in CaF_2 crystals have been measured at room and liquid-nitrogen temperatures. Their spectra are similar to each other in the general location of their absorption bands. Both spectra consist of: (i) $4f\rightarrow 5d$ bands, between about 24 000 cm^{-1} and about 50 000 cm^{-1}, due to isolated RE^{2+} with crystal field strength $\sim$17 000 cm^{-1} between e_g and t_{2g} bands; (ii) $4f\rightarrow 5d$ bands, shifted $\sim$9 000 cm^{-1} to higher energy, due to RE^{2+} ions surrounded by RE^{3+} neighbors; (iii) a $4f\rightarrow 6p$ broad and weak band of Eu^{2+} in CaF_2 with maximum at $\sim$71 000 cm^{-1}; and (iv) $4f\rightarrow 5d$ bands above $\sim$64 000 cm^{-1} due to isolated RE^{3+} and cluster-ion RE^{3+}. The structure in the absorption spectra of both isolated $RE^{3+}(4f^n)$ and $RE^{3+}(4f^n)$ ions can be interpreted as formed through interaction between a $5d$ electron having e_g or t_{2g} crystal field symmetry and electrons in the ground multiplet of the $4f^{n-1}$ core.

I. INTRODUCTION

As a direct approach to the study of interconfigurational transitions of rare-earth (RE) ions in solids, we have previously presented the uv absorption spectra of two simple trivalent rare-earth ions, $Ce^{3+}(4f^1)$ (Ref. 1) and $Pr^{3+}(4f^2)$ (Ref. 2), in alkaline-earth fluorides. Their spectra show three types of transitions in the order of increasing energy: (a) $4f\rightarrow 5d$ bands, (b) a broad and weak $4f\rightarrow 6s$ band, and (c) the charge transfer of F^- $(2p^6)\rightarrow RE^{3+}$ $(6s)$ appearing as the red shift of the absorption edge of the host crystal.

For comparison with the work on RE^{3+}, we present here the uv-absorption spectra of two common RE^{2+} ions, $Eu^{2+}(4f^7)$ and $Yb(4f^{14})$, in CaF_2. Contrary to most of RE ions in solids, europium and, to a lesser extent, ytterbium are usually in the divalent rather than trivalent state because of their tendency to complete the half, Eu^{2+} $(4f^7)$, and full, Yb^{2+} $(4f^{14})$, $4f$ shell, respectively. Their spectra are stable and perhaps also simple because no strenuous reduction process[3,4] is required to convert RE^{3+} to RE^{2+}. Furthermore, the energy gaps in the ground multiplet of $4f^{n-1}$ are among the narrowest for Eu^{2+}, $4f^{n-1}=4f^6$, and the widest for Yb^{2+}, $4f^{n-1}=4f^{13}$. The uv-absorption spectra of Eu^{2+} and Yb^{2+}, therefore, provide simple examples to interpret the structure[5] of $4f^n\rightarrow 4f^{n-1}5d$ bands and

* Work partially supported by the McDonnell Douglas Astronautics Company-Western Division under the Independent Research and Development Program.

[1] E. Loh, Phys. Rev. **154**, 270 (1967).

[2] E. Loh, Phys. Rev. **158**, 273 (1967).

[3] J. L. Merz and P. S. Pershan, Phys. Rev. **162**, 217 (1967); **162**, 235 (1967); J. L. Merz, Ph.D. thesis, Harvard University, 1966 (unpublished). Available as Technical Report No. 514, Office of Naval Research, NR-372-012, and references therein.

[4] D. S. McClure and Z. Kiss, J. Chem. Phys. **39**, 3251 (1963).

[5] E. Loh, Phys. Rev. **175**, 533 (1968).